J Mol Model (2014) 20:2536
DOI 10.1007/s00894-014-2536-6

ORIGINAL PAPER

The structure, stability, and electronic properties of ultra-thin BC_2N nanotubes: a first-principles study

Yue Wang · Juan Zhang · Gang Huang · Xinhua Yao · Qingyi Shao

Received: 11 June 2014 / Accepted: 17 November 2014 / Published online: 2 December 2014

Abstract Rapid developments of the silicon electronics industry have close to the physical limits and nanotube materials are the ideal materials to replace silicon for the preparation of next generation electronic devices. Boron-carbon-nitrogen nanotubes (BCNNT) can be formed by joining carbon nanotube (CNT) and boron nitride nanotube (BNNT) segments, and BC_2N nanotubes have been widely and deeply studied. Here, we employed first-principles calculations based on density function theory (DFT) to study the structure, stability, and electronic properties of ultra thin (4 Å diameter) BC_2N nanotubes. Our results showed that the cross sections of BC_2N nanotubes can transform from round to oval when CNT and BNNT segments are parallel to the tube axis. It results when the curvature of BNNT segments become larger than CNT segments. Further, we found the stability of BC_2N nanotubes is sensitive to the number of B-N bonds, and the phase segregation of BNNT and CNT segments is energetically favored. We also obtained that all (3,3) BC_2N nanotubes are semiconductor, whereas (5,0) BC_2N nanotubes are conductor when CNT and BNNT segments are perpendicular to the tube axis; and semiconductor when CNT and BNNT segments are parallel to the tube axis. These electronic properties are abnormal when compared to the relative big ones.

Keywords BC_2N nanotubes · Electronic properties · First-principles · Stability · Structure

Introduction

In the past few decades, the progress of silicon electronics industry was based on producing smaller, faster, and more powerful devices, which requires denser integrated circuits (have more transistors on a single chip) and in turn requires much smaller transistors. Much higher transistor density on a single chip means much faster circuit performance, but it requires smaller materials (nano materials) for the preparation of smaller transistors, and nanotube materials have been considered as one of the ideal materials for the preparation of next generation nano electronic devices. Nanotube materials, especially for carbon nanotubes (CNT) [1], have smaller volume, unique quasi-one-dimensional atomic structure, novel physical properties, and supports rapid switching in comparison with the conventional silicon material [2]. So using it to replace silicon can produce much smaller, faster, and more energy efficient transistors. Recently, scientists have made some significant achievements in the experiment about the practical application of carbon nanotubes [3–6]. It means the electronic components and electronic products which were prepared using carbon nanotubes will come true in the near future.

CNT with different tubular diameter or chirality will have different electronic properties (conductor or semiconductor) [7, 8]. On the other hand, boron nitrogen nanotubes (BNNT) show a much more uniform electrical behavior with an almost constant band gap of about 5.5 eV, independent of their diameter and chirality [9]. So the electronic properties of boron-carbon-nitrogen nanotubes (BCNNT), which are composed of CNT and BNNT segments, may be controlled by changing the relative ratio and configurations of CNT and BNNT segments. In addition, BCNNT have been successfully synthesized using chemical vapor deposition [10], arc-discharge [11], atom transfer radical polymerization [12], laser vaporization [13], and spray pyrolysis [14] techniques. As an important member of the BCNNT family, BC_2N has been widely and deeply studied. Pan et al. [15] showed that the strain energy of the BC_2N nanotubes depends on the diameter and the electronic properties are closely related to both the

Y. Wang · J. Zhang · G. Huang · X. Yao · Q. Shao (✉)
Laboratory of Quantum Engineering and Quantum Materials, School of Physics and Telecommunication Engineering, South China Normal University, Guangzhou 510006, China
e-mail: qyshao@163.com

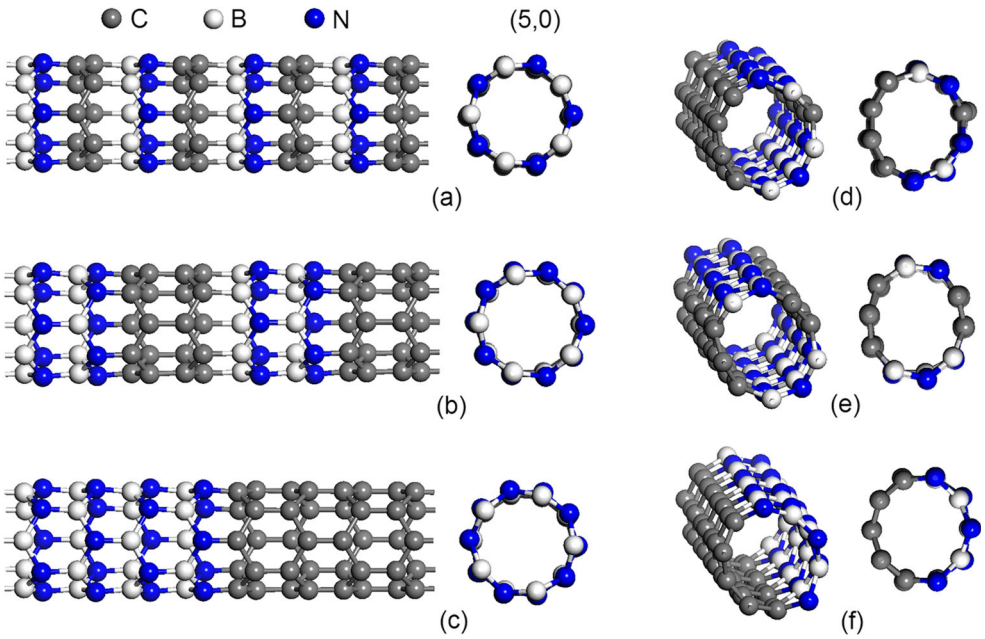

Fig. 1 Different configurations of (5,0) BC_2N nanotubes. The tubes in (**a**) to (**c**) are perpendicularly arranged and labeled with ZZ-a, ZZ-b, and ZZ-c, respectively, including the lateral views (*left*) and the cross sections (*right*). The tubes in (**d**) to (**f**) are parallel arranged and labeled with ZZ-d, ZZ-e, and ZZ-f, respectively, including the oblique drawing (*left*) and the cross section (*right*)

diameter and chirality of the tube. Investigating the adsorption behaviors of atomic and molecular hydrogen on BC_2N nanotubes indicated that BC_2N nanotubes can exhibit donor or acceptor characteristics depending on the adsorption site for the H [16]. Si doped BC_2N nanotubes have been found to not only strongly adsorb the H_2CO molecule, but also may effectively detect its presence because of the increase in the electric conductivity of the tube [17]. Theoretical study found the preservation of electronic properties of BC_2N coupled with the enhancement of solubility renders their chemical modification with either NH_3 or amino functional groups to be a way for the purification of BC_2N nanotubes [18]. Baei et al. [19] showed that the properties of BC_2N nanotube can be controlled by the proper external electric field for use in nanoelectronic circuits. Peyghan et al. [20] showed Al-doped BC_2N nanotubes can largely improve the reactivity to HCN. Rupp et al. [21] found that silicon impurity has lower formation energy for the BC_2N nanotubes as compared with Si-doped CNT and BNNT, and BC_2N nanotubes have different electronic properties depending on different position of silicon doped. Theoretical studies of BC_2N nanotubes indicated that, in general, the electronic properties of BC_2N nanotubes strongly depend on the geometrical arrangements of CNT and BNNT segments [22–24], and there is a tendency toward

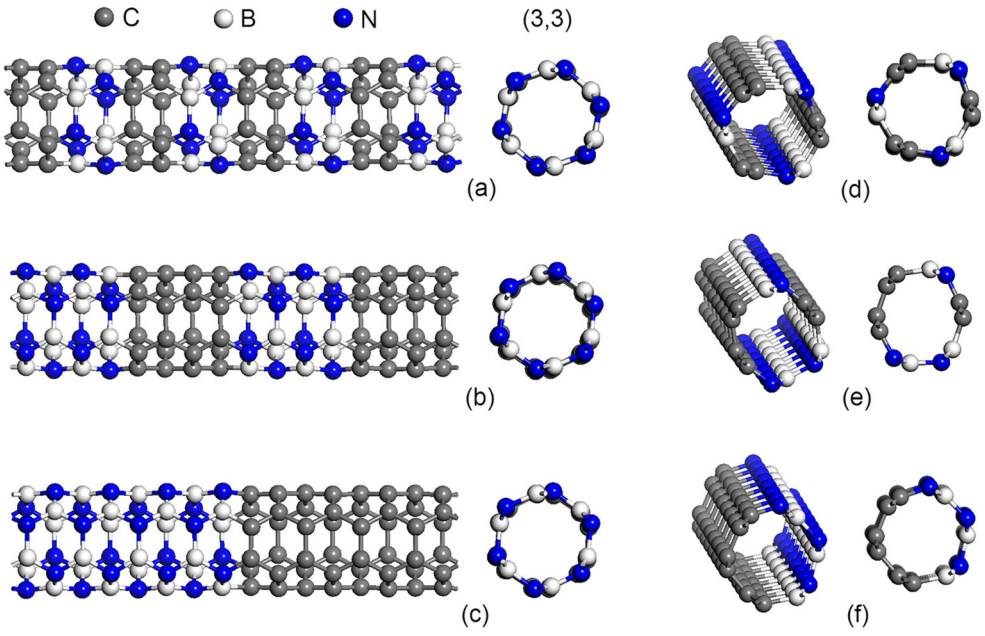

Fig. 2 Different configurations of (3,3) BC_2N nanotubes. The tubes in (**a**) to (**c**) are perpendicularly arranged and labeled with AC-a, AC-b, and AC-c, respectively, including the lateral views (*left*) and the cross sections (*right*). The tubes in (**d**) to (**f**) are parallel arranged and labeled with AC-d, AC-e, and AC-f, respectively, including the oblique drawing (*left*) and the cross section (*right*)

Table 1 Calculated average bond lengths of the studied BC_2N nanotubes. ZZ-original corresponding to the original bond length of BC_2N nanotubes for ZZ-d, ZZ-e, and ZZ-f; AC-original corresponding to the original bond length of BC_2N nanotubes for AC-d, AC-e, and AC-f. All lengths are given in Å

Configuration	C-C⊥	C-C∥	C-B⊥	C-B∥	C-N⊥	C-N∥	B-N⊥	B-N∥
ZZ-d	1.444	1.389	1.544	–	1.428	–	1.488	1.437
ZZ-e	1.431	1.406	1.542	–	1.431	–	1.498	1.434
ZZ-f	1.449	1.400	1.560	–	1.440	–	1.476	1.434
ZZ-original	1.453	1.408	1.453	–	1.453	–	1.453	1.408
AC-d	–	1.424	1.534	–	1.401	–	–	1.457
AC-e	1.454	1.424	1.541	–	1.406	–	1.438	1.458
AC-f	1.456	1.426	1.550	–	1.410	–	1.441	1.457
AC-original	1.440	1.431	1.440	–	1.440	–	1.440	1.431

the phase segregation of CNT and BNNT segments [23, 24]. However, to our knowledge, there has been no detailed report on ultra-small diameter BC_2N nanotubes.

In this paper, we performed first-principles calculations to study the structure, stability, and electronic properties of ultra small diameter (4 Å) BC_2N nanotubes from different configurations. For ultra thin nanotubes, CNT with 4 Å diameter have been proved stable [25, 26] and can be prepared in the central core of multiwall carbon nanotubes (MWCNT) or in a channel [27–29]. Much smaller devices require it has much higher levels of integration, which in turn requires much smaller size of materials to prepare much smaller transistors. Therefor, the electronic properties of ultra-thin BC_2N nanotubes should be understood when used in the preparation of much smaller nano electronic devices (such as nano switch, nano transistors, and so on). The theoretical investigation about the modification of ultra thin CNT has also been reported [30]. Moreover, for nanotubes, the extremely small diameter of tube means that the simple band-folding picture can no longer predict the electronic structure reliably. For example, single walled carbon nanotubes (SWCNT) (5,0) should be a semiconductor according to zone folding, but it turns into a metal as a consequence of large curvature effect [31]. This means the ultra-small diameter nanotubes have some abnormal electronic properties when compared with the relative big ones. So we also have interest to investigate whether the electronic properties of ultra-small diameter BC_2N nanotubes are also distinct from the relative big ones.

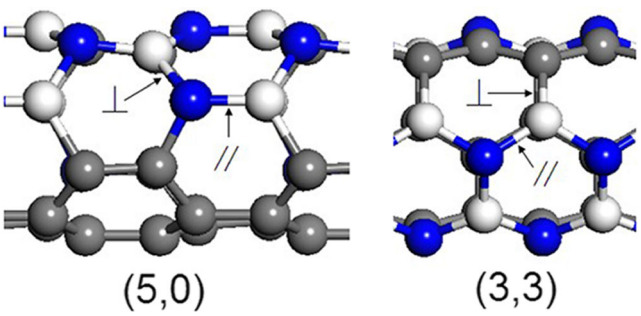

Fig. 3 The bond styles of the studied zigzag and armchair BC_2N nanotubes. ⊥ represents that the bond is perpendicular to the tube axis while ∥ means parallel to the tube axis

Theoretical methods

We used the code DMol^3 based on density-functional theory (DFT) [32, 33], available from Accelrys Inc. In this code, each electronic wave function was expanded into a localized atom-centred basis set with each basis function defined numerically on a dense radial grid. For the exchange and correlation term, the generalized gradient approximation (GGA) was used as proposed by Perdew, Burke, and Ernzerhof (PBE) [34]. The electronic wave functions are expanded in a double numeric polarized (DNP) basis set with an orbital cutoff of 4.5 Å. The type of treatments of core electrons is all electron forms. Geometry optimization was performed with the self-consistent field (SCF) tolerance of $1.\ 0\times10^{-5}$ Ha (1 Ha= 27.2114 eV), the maximum force of 0.002 Ha/Å and the maximum displacement of 0.005 Å. The k-points are set 1×1×6 for all structures, according to the Monkhorst–Pack approximation [35]. Calculations using more k-points did not have any significant effects for the results.

In this work, zigzag (5,0) (see Fig. 1) and armchair (3,3) (see Fig. 2) BC_2N nanotubes were chosen as models to research. A one-dimensional periodic boundary condition was applied along the tube axis, in which periodically repeating tetragonal supercells with lattice constants a, b, and c were used, and both a and b are long enough (12 Å) to ensure negligible interaction between the tubes. There exist two distinct structural combinations of CNT segments with BNNT segments for (5,0) and (3,3) BC_2N nanotubes: (1) the segments of CNT and BNNT perpendicular to the tube axis, and (2) the segments of CNT and BNNT parallel to the tube axis. We use binding energy (E_b) to study the stability of BC_2N nanotubes, and E_b was defined by the following equation [23, 24]:

$$Eb = Etot - n(B)\mu(B) - n(C)\mu(C) - n(N)\mu(N), \quad (1)$$

where E_{tot} is the total energy of the BC_2N nanotubes from the supercell calculation; μ(B), μ(C), and μ(N) are the chemical potentials of single B, C, and N atoms, respectively; n(B), n(C), and n(N) are the number of B, C, and N atoms in BC_2N nanotubes, respectively.

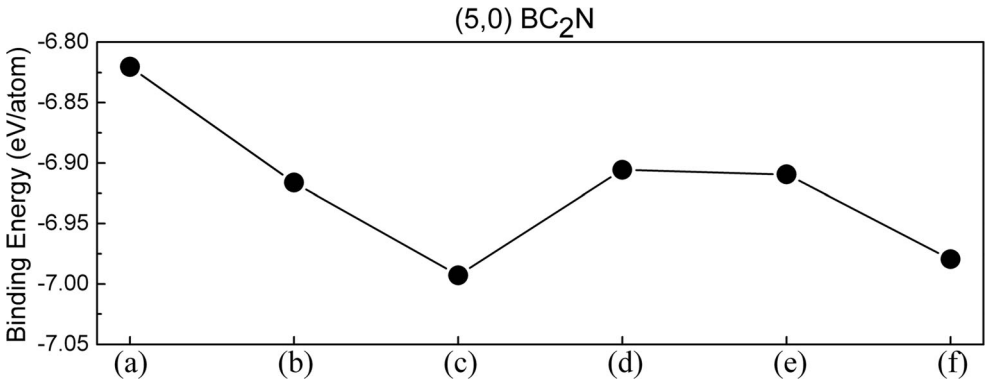

Fig. 4 Calculated binding energies (E_b) for the studied zigzag (5,0) BC_2N nanotubes, labeled **a** ZZ-a, **b** ZZ-b, **c** ZZ-c, **d** ZZ-d, **e** ZZ-e, and **f** ZZ-f

Results and discussion

Structure

In Figs. 1 and 2, we showed the final structures of the studied zigzag (5,0) and armchair (3,3) BC_2N nanotubes that have been geometry optimized. It can be seen from Figs. 1 and 2 that the cross sections of BC_2N nanotubes are still circular when the segments of CNT and BNNT are perpendicular to the tube axis, regardless of (5,0) or (3,3) BC_2N nanotubes. However, when the segments of CNT and BNNT are parallel to the tube axis the circular cross sections of BC_2N nanotubes were destroyed after geometry optimized. As shown in Figs. 1 and 2, the final structure of BC_2N nanotubes for ZZ-d, ZZ-e, and AC-e have an oval cross section, tube ZZ-f also has an oval cross section, but not very obvious. For tube AC-d, BNNT segment has a raised structure on the surface of tube.

In order to further study the structure of (5,0) and (3,3) BC_2N nanotubes, we calculated the average bond length of BC_2N nanotubes for ZZ-d, ZZ-e, ZZ-f, AC-d, AC-e, and AC-f that have been geometry optimized and their original bond length (see Table 1). In Fig. 3, we defined two styles of bond for zigzag and armchair nanotubes, $\perp$ represents that the bond is perpendicular to the tube axis while $\parallel$ means parallel to the tube axis. As shown in Table 1, original BC_2N nanotubes (have not been geometry optimized) have uniform bond length for the same bond style and a circular cross section, regardless of (5,0) or (3,3) BC_2N nanotubes. However, after BC_2N nanotubes have been optimized, the original symmetry was destroyed. For BC_2N nanotubes ZZ-d, ZZ-e, and ZZ-f, the bond lengths of C-B$\perp$ and B-N$\perp$ become larger than C-C$\perp$, especially for C-B$\perp$, which is approximately 0.1 Å (about 7 %) larger than C-C$\perp$. It results in a decrease in the curvature of the CNT segments and an increase in the curvature of the BNNT segments, so an elliptical cross section was formed. For BC_2N nanotubes AC-d and AC-e, the bond length of C-B$\perp$ (1.534 Å for AC-d and 1.541 Å for AC-e) becomes obviously larger than its original length (1.440 Å), and the length of other bonds are almost not changed. In addition, tube AC-d has three CNT segments and three BNNT segments, CNT segments and BNNT segments are arranged alternately, so BNNT segments have a raised structure on the surface of tube AC-d. For tube AC-e, which has two CNT segments and two BNNT segments with one BNNT (CNT) segment at the opposite of another BNNT (CNT) segment, so the cross section of tube AC-e converted from round into oval.

Stability

We have calculated the binding energies of (5,0) (see Fig. 4) and (3,3) (see Fig. 5) BC_2N nanotubes to study their stability. As shown in Figs. 4 and 5, our results shown that the binding energies of (5,0) and (3,3) BC_2N nanotubes are negative,

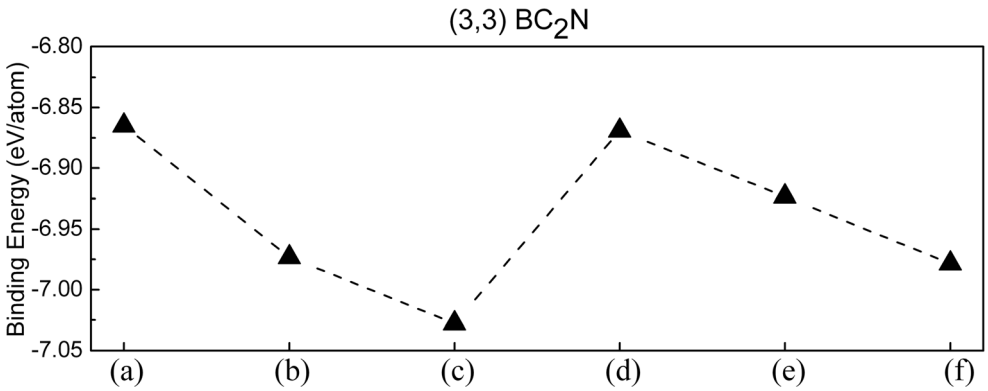

Fig. 5 Calculated binding energies (E_b) for the studied armchair (3,3) BC_2N nanotubes, labeled **a** AC-a, **b** AC-b, **c** AC-c, **d** AC-d, **e** AC-e, and **f** AC-f

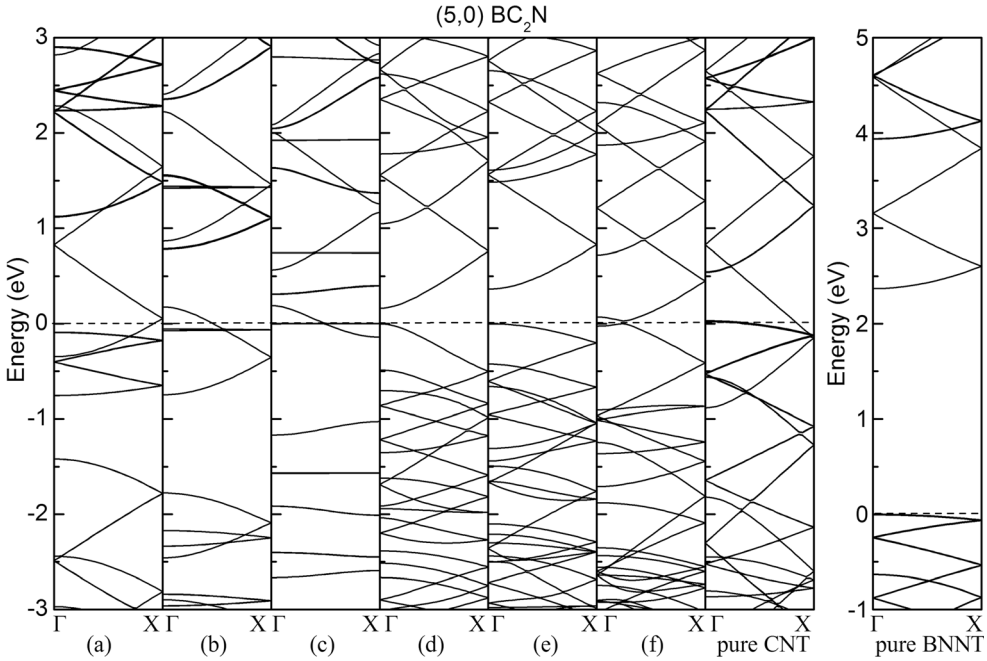

Fig. 6 Calculated band structures for (5,0) BC_2N nanotubes labeled **a** ZZ-a, **b** ZZ-b, **c** ZZ-c, **d** ZZ-d, **e** ZZ-e, and **f** ZZ-f. The Fermi level is set at zero

indicating the ultra small diameter (4 Å) BC_2N nanotubes are energetically stable. We also found that with the increasing numbers of B-N bonds, there is a decrease of binding energies, regardless of (5,0) or (3,3) BC_2N nanotubes. For instance, for (5,0) BC_2N nanotubes, from tubes ZZ-a to ZZ-c, Fig. 1 shows the number of B-N bonds in these tubes is increased and Fig. 4 shows their binding energies are decreased in turn. Tubes ZZ-d and ZZ-e have the same number of B-N bonds (see Fig. 1) and almost the same binding energies (see Fig. 4), And tube ZZ-f has a larger number of B-N bonds and more low binding energy in comparison with ZZ-d and ZZ-e (see Figs. 1 and 4). For (3,3) BC_2N nanotubes (see Figs. 2 and 5), the binding energies decrease gradually with the increasing number of B-N bonds, from tubes AC-a to AC-c and AC-d to AC-f. All of the above results indicate that the increase in the segregation of the CNT and BNNT segments (the increase in the number of B-N bonds) of BC_2N nanotubes tends to increase the stability (decrease the binding energies) of BC_2N nanotubes. It is because the energy of B-N bond is larger than C-C bond [36], so it is an exothermic process to break a C-C bond and build a new B-N bond at the same time. Leading to BC_2N nanotubes with more B-N bonds will be more stable.

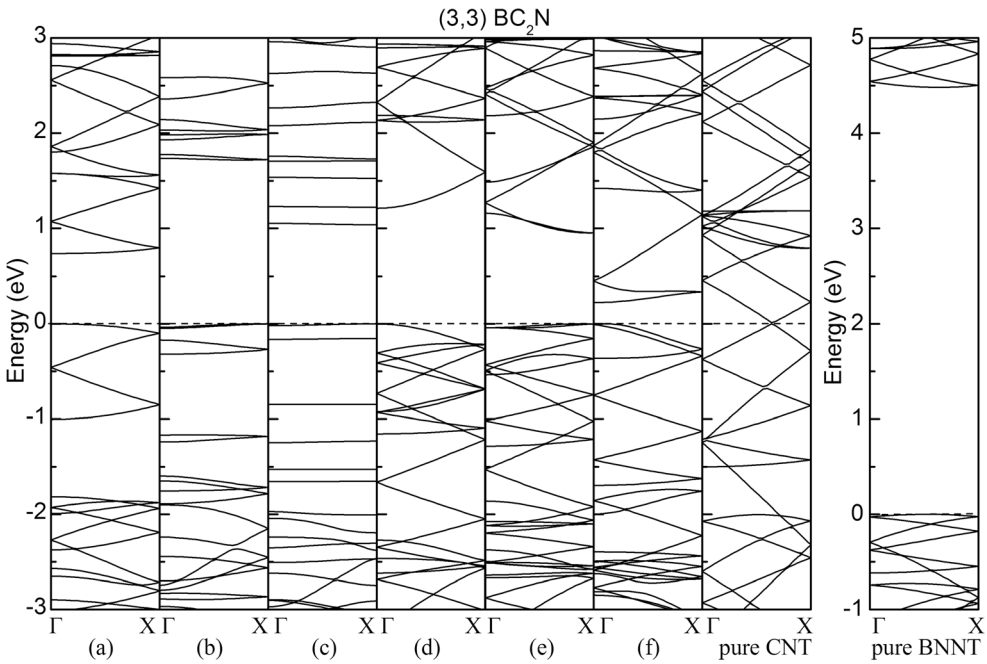

Fig. 7 Calculated band structures for (3,3) BC_2N nanotubes labeled **a** AC-a, **b** AC-b, **c** AC-c, **d** AC-d, **e** AC-e, and **f** AC-f. The Fermi level is set at zero

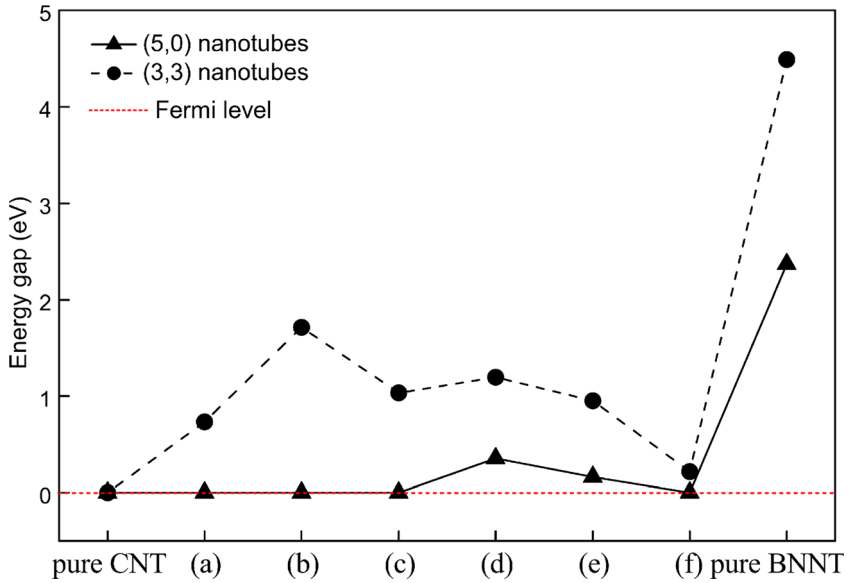

Fig. 8 Energy gap of the BC_2N nanotubes, pure CNT, and pure BNNT. The Fermi level is set at zero

Electronic properties

We have calculated the band structure of (5,0) and (3,3) BC_2N nanotubes (see Figs. 6 and 7, respectively). As shown in Figs. 6 and 7, our calculated results agree with previous studies that both (5,0) and (3,3) CNT are conductor [31], whereas both (5,0) and (3,3) BNNT are semiconductor [9]. However, for BC_2N nanotubes, our results have some differences in comparison with the relative big ones in previous studies.

Previous investigations of BC_2N nanotubes with CNT and BNNT segments perpendicular to tube axis found that zigzag (8,0) and (9,0) BC_2N nanotubes are semiconductor [22, 23], and An et al. found that zigzag (8,0) BC_2N nanotubes can be conductor or semiconductor depending on different configurations [24]. However, our results are abnormal when compared to the relative big ones in previous studies. From Fig. 6, we can see that BC_2N nanotubes ZZ-a, ZZ-b, and ZZ-c are all conductor with significant electronic states populated at Fermi level. It may be due to the large curvature of tube, like SWCNT (5,0) which should be semiconducting according to zone folding, transforms into metallic as a consequence of large curvature effect [33]. For armchair BC_2N nanotubes, previous studies found that all (6,6) BC_2N nanotubes are semiconductor [23, 24]. Our study has the same result with previous studies, as shown in Fig. 7, BC_2N nanotubes AC-a, AC-b, and AC-c are semiconductor with energy gaps of 0.735, 1.714, and 1.034 eV, respectively.

It can be seen from Figs. 6 and 7 that BC_2N nanotubes AC-d, AC-e, ZZ-d, and ZZ-e with the CNT and BNNT segments parallel to the tube axis are semiconductor with significant energy gap. For BC_2N nanotubes AC-f and ZZ-f, which correspond to continuous segments of CNT and BNNT, with each segment corresponding to one-half of the tube. Our result shows tube ZZ-f is a conductor (see Fig. 6) while AC-f is a semiconductor with an energy gap of 0.218 eV (see Fig. 7). However, previous studies have the opposite results that zigzag BC_2N nanotubes ((8,0), (10,0), and (12,0)) with the configuration as tube ZZ-f always having a semiconductor character [23, 24, 37], and armchair BC_2N nanotubes ((4,4), (5,5), (6,6), and (10,10)) with the configuration as tube AC-f would always be conductor [22–24, 37, 38]. It means that the electronic properties of ultra thin (4 Å diameter) (5,0) and (3,3) BC_2N nanotubes are abnormal in comparison with the relative big ones.

As shown in Fig. 8, we found zigzag (5,0) BC_2N nanotubes can be conductor or semiconductor depending on different configurations of CNT and BNNT segments. However, all armchair (3,3) BC_2N nanotubes are semiconductor, and the energy gaps are tunable when the segments of CNT and BNNT parallel to the tube axis, it decreases with the increasing number of B-N bonds. Therefore, we can conclude that the electronic properties of ultra-thin BC_2N nanotubes have a direct relationship with the chirality of tubes and the configurations of CNT and BNNT segments, and are different from the relative big ones in previous investigations.

In order to further understand the electronic properties of each BC_2N nanotubes, we investigate the total density of states (DOS) and projected density of states (PDOS) (see Figs. 9 and 10). Considering that the electronic properties depend chiefly on the electronic states near the Fermi level, we only care about the electronic states around the Fermi level. As shown in Fig. 9, for metallic tube ZZ-a, ZZ-b and ZZ-c, the DOS near Fermi level is mainly contributed by C atom and small part by B and N atoms, and there are also a peak of DOS near the Fermi level locate at different position (ZZ-a about at −0.2 eV, ZZ-b about at −0.1 eV and ZZ-c at the position of Fermi level). For semiconducting tube ZZ-d, the

conduction band bottom mainly comes from C atom and partly from B atom; the valence band top mainly comes from C atom and partly from N atom. The DOS of tube ZZ-e (semiconductor) and ZZ-f (conductor) near Fermi level are almost all contributed by C atom, B and N atoms contribute nothing to it. Figure 10 shows the DOS and PDOS of armchair (3,3) BC_2N nanotubes. Although all armchair (3,3) BC_2N nanotubes are semiconductor, it is different for the PDOS near Fermi level between perpendicular arrangement and parallel arrangement tubes. For perpendicular arrangement tubes AC-a, AC-b and AC-c, the DOS near Fermi level basically come from C atom. For parallel arrangement tubes AC-d, AC-e and AC-f, the major contribution of both conductor band bottom and valence band top come from C atom, and a minority from N and B atom for conductor band bottom and valence band top, respectively. We also found that there was a peak of DOS

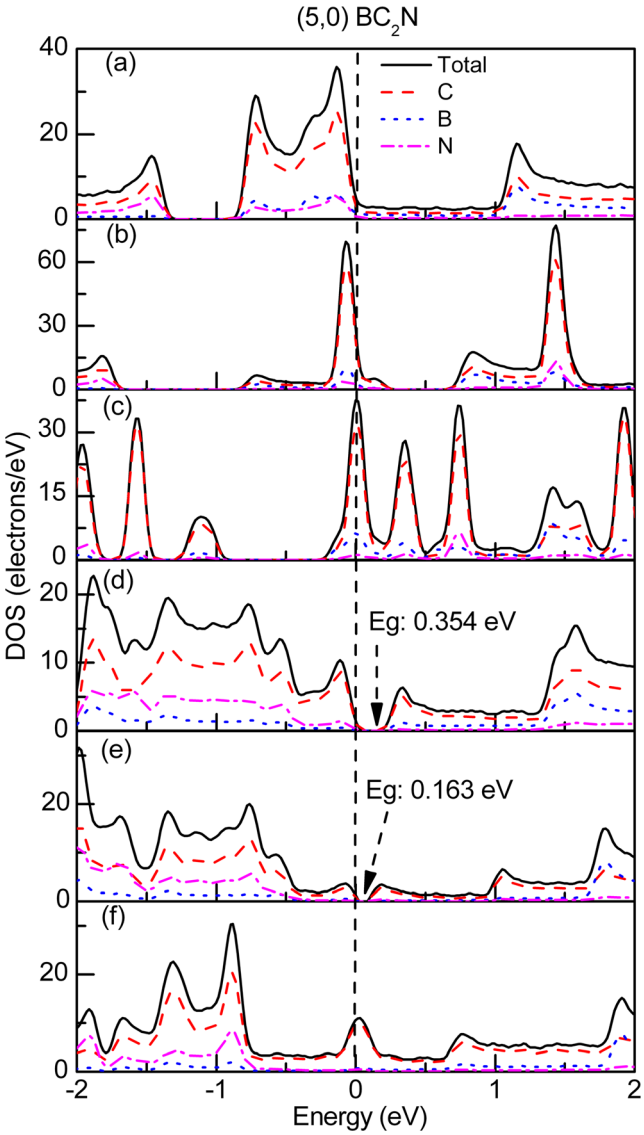

Fig. 9 The DOS and PDOS of (5,0) BC_2N nanotubes. The energy gap (Eg) and Fermi level is indicated by *arrows* and *dashed line*, respectively

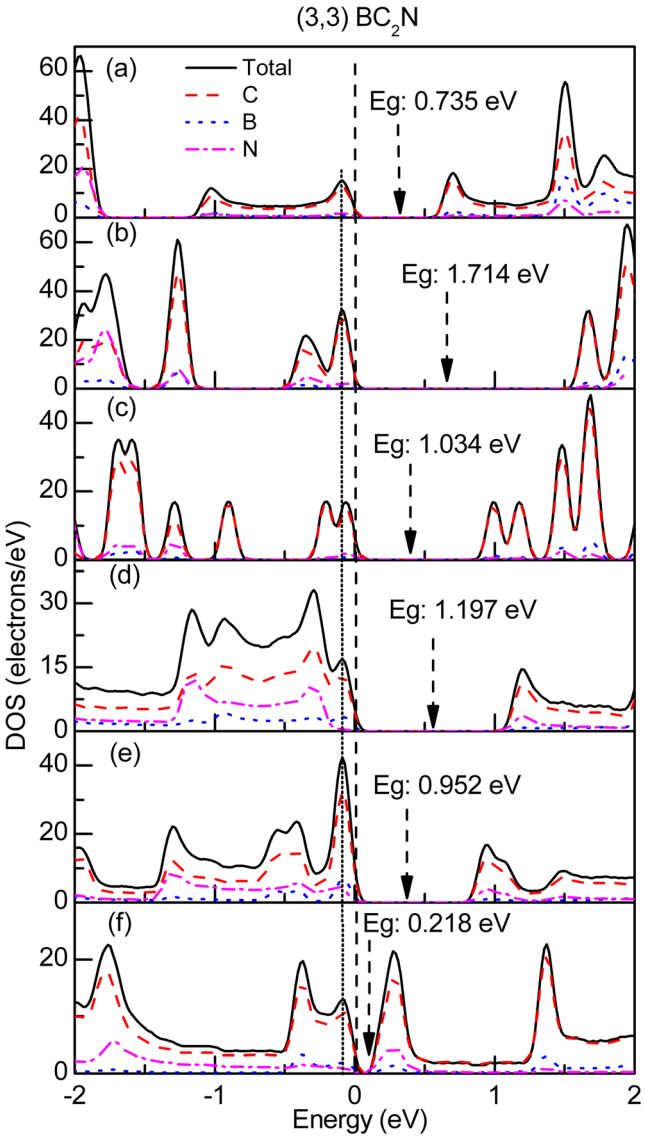

Fig. 10 The DOS and PDOS of (3,3) BC_2N nanotubes. The energy gap (Eg) and Fermi level is indicated by *arrows* and *dashed line*, respectively

bellow Fermi level located at about −0.1 eV for all (3,3) BC_2N nanotubes except for tube AC-c (see the short dashed line in Fig. 10).

Conclusions

In conclusion, we have investigated the structure, energy, and electronic properties of ultra thin (4 Å diameter) BC_2N nanotubes formed by joining CNT and BNNT segments with different geometrical arrangements through first-principles calculations. We found that an oval cross section was obtained for BC_2N nanotubes when CNT and BNNT segments are parallel to the tube axis. Further, ultra small diameter (4 Å) BC_2N nanotubes are energetically stable, and present more stable with more B-N bonds. Finally, we also showed that the

electronic properties (energy gap) of BC_2N nanotubes are tunable and distinct from the relative big ones. These findings of ultra thin (4 Å diameter) BC_2N nanotubes may have potential application in future design of ultra small and powerful nano electronic devices.

Acknowledgments This work was supported by the Natural Science Foundation of the Fujian Province of China (grant no. A0220001). We acknowledge the high-performance computing platform of South China Normal University for financial support.

References

1. Iijima S (1991) Nature 354:56
2. Popov VN (2004) Mater Sci Eng R 43:61–102
3. Derycke V, Martel R, Appenzeller J, Avouris PH (2001) Nano Lett 1: 453–456
4. Bachtold A, Hadley P, Takeshi N, Dekker C (2001) Science 294: 1317–1320
5. Chen AQ, Shao QY, Li Z (2011) J Nanoparticle Res 13:2275–2283
6. Shulaker MM, Hills G, Patil N, Wei H, Chen HY, Philip Wong HS, Mitra S (2013) Nature 501:526–530
7. Wildöer JWG, Venema LC, Rinzler AG, Smalley RE, Dekker C (1998) Nature 391:59–62
8. Odom TW, Huang JL, Kim P, Lieb CM (1998) Nature 391:62–64
9. Bkase X, Rubio A, Louie SG, Cohen ML (1994) Europhys Lett 28: 335–340
10. Wang WL, Bai XD, Liu KH, Xu Z, Golberg D, Bando Y, Wang EG (2006) J Am Chem Soc 128:6530–6531
11. Weng-Sieh Z, Zettl A, Gronsky R (1995) Phys Rev B 51:11229–11231
12. Zhi CY, Bando Y, Tang CC, Kuwahara H, Golberg D (2007) J Phys Chem C 111:1230–1233
13. Enouz S, Stéphan O, Cochon JL, Colliex C, Loiseau A (2007) Nano Lett 7:1856–1862
14. Yadav RM, Dobal PS (2012) J Nanoparticle Res 14:1155
15. Pan H, Feng YP, Lin JY (2006) Phys Rev B 74:045409
16. Rossato J, Raierle RJ, Schmidt TM, Fazzio A (2008) Phys Rev B 77: 035129
17. Noei M, Ahmadi Peyghan A (2013) J Mol Model 19:3843–3850
18. Beheshtian J, Ahmadi Peyghan A (2013) J Mol Model 19:2211–2216
19. Baei MT, Peyghan Peyghan A, Moghimi M, Hashemian S (2013) J Mol Model 19:97–107
20. Peyghan Peyghan A, Hadipour NL, Bagheri Z (2013) J Phys Chem C 117:2427–2432
21. Rupp CJ, Rossato J, Baierle RJ (2009) J Chem Phys 130: 114710
22. Choi J, Kim YH, Chang HJ, Tománek D (2003) Phys Rev B 67: 125421
23. Machado M, Kar T, Piquini P (2011) Nanotechnology 22:205706
24. An W, Turner CH (2010) J Phys Chem Lett 1:2269–2273
25. Cabria I, Mintmire JW, White CT (2003) Phys Rev B 67:121406
26. Peng LM, Zhang ZL, Xue ZQ, Wu QD, Gu ZN, Pettifor DG (2000) Phys Rev Lett 85:3249–3252
27. Qin LC, Zhao XL, Hirahara K, Miyamoto Y, Ando Y, Iijima S (2000) Nature 408:50–50
28. Wang N, Tang ZK, Li GD, Chen JS (2000) Nature 408:50–51
29. Hayashi T, Kim YA, Matoba T, Esaka M, Nishimura K, Tsukada T, Endo M, Dresselhaus MS (2003) Nano Lett 3:887–889
30. Xia J, Shao CR, Wang T, Zhang J, Shao QY (2013) Chem Phys Lett 579:127–131
31. Liu HJ, Chan CT (2002) Phys Rev B 66:115416
32. Delley B (1990) J Chem Phys 92:508–517
33. Delley B (2000) J Chem Phys 113:7756–7764
34. Perdew JP, Burke K, Ernzerhof M (1996) Phys Rev Lett 77:3865–3868
35. Monkhorst HJ, Pack JD (1976) Phys Rev B 13:5188–5192
36. Nozaki H, Itoh S (1996) J Phys Chem Solids 57:41–49
37. Du A, Chen Y, Zhu ZH, Lu GQ, Smith SC (2009) J Am Chem Soc 131:1682–1683
38. Zhang ZY, Zhang ZH, Guo WL (2009) J Phys Chem C 113:13108–13114